Journal of Mechanics in Medicine and Biology
Vol. 11, No. 1 (2011) 205–219

DOI: 10.1142/S0219519411003983

World Scientific
www.worldscientific.com

FLUID DYNAMICS ANALYSIS OF SHEAR STRESS ON NERVE ENDINGS IN DENTINAL MICROTUBULE: A QUANTITATIVE INTERPRETATION OF HYDRODYNAMIC THEORY FOR DENTAL PAIN

M. LIN*, Z. Y. LUO†, B. F. BAI†, F. XU*,‡,§,‖ and T. J. LU*,¶,‖

*Biomedical Engineering and Biomechanics Center, School of Aerospace
Xi'an Jiaotong University, Xi'an 710049, P. R. China

†State Key Laboratory of Multiphase Flow in Power Engineering
Xi'an Jiaotong University
Xi'an 710049, P. R. China

‡HST-Center for Biomedical Engineering
Department of Medicine, Brigham and Women's Hospital
Harvard Medical School, Boston, MA, USA
§fxu2@rics.bwh.harvard.edu
¶tjlu@mail.xjtu.edu.cn

Received 19 October 2010
Revised 5 December 2010
Accepted 7 December 2010

Noxious thermal and/or mechanical stimuli applied to dentine can cause fluid flow in dentinal microtubules (DMTs). The fluid flow induces shear stress (SS) on intradental nerve endings and may excite pulpal mechanoreceptors to generate dental pain sensation. There exist numerous studies on dental thermal pain, but few are mathematical. For this, we developed a computational fluid dynamics (CFD) model of dentinal fluid flow (DFF) in innervated DMTs. Based on this model, we systematically investigated the effects of various parameters (e.g., biological structure, DFF velocity, and fluid properties) on the SS experienced by intradental nerve endings and thus provide a quantitative interpretation to the hydrodynamic theory. The dimensions of biological structures, odontoblastic process (OP) movement, dentinal fluid velocity, and viscosity were found to have significant influences on the SS while dentinal fluid density showed negligible influence under conditions studied. The results indicate that: (i) dental pain study of animal models may not be directly applied to human being and the results may even vary from one person to another and (ii) OP movement caused by DFF changes the dimension of the space for the fluid flow, affecting thus the SS on nerve endings. The present work enables better understanding of the mechanisms underlying dental pain sensation and quantification of dental pain intensity resulted from clinical procedures such as dentine sensitivity testing and dental restorative processes.

Keywords: Dentinal fluid flow; shear stress; dentinal microtubule; mechanoreceptor; computational fluid dynamics.

‖Corresponding authors.

1. Introduction

Dental thermal pain is a common problem in daily life and dentistry,[1] especially when high-energy output instruments (e.g. dental lasers[2,3] and light-polymerizing units[4–6]) are employed in clinics. Three hypotheses have been proposed to explain the transduction process of dental pain sensation,[7] including the neural theory, the odontoblastic transduction theory, and the hydrodynamic theory. Amongst the three hypotheses, the hydrodynamic theory has been widely accepted as supported by existing experimental evidences.[8–10] The hydrodynamic theory assumes that dentinal fluid flow (DFF) within dentinal microtubules (DMTs) Figs. 1(a)–1(b) induced by noxious stimuli may activate mechanoreceptors located within DMTs or at the pulp-dentine junction resulting in pain sensation,[16–19] Fig. 1(c). One supporting evidence of the hydrodynamic theory is that the sensory response of teeth to thermal agitation was elicited before a temperature change was detected in the pulp–dentine junction, where most sensory structures are located.[20]

Shear stress (SS) has been shown to play an important role in dental pain sensation. Stimulation applied on tooth can initiate DFF[8,21,22] activating mechanoreceptors, resulting in dental pain sensation.[17–19,24,25] The role of SS in dental pain transduction process can be further confirmed by the correlation between DFF velocity in DMTs and intradental nerve firing rate,[23,26] where a higher rate of DFF may induce a larger SS on the mechanoreceptors, resulting in increased nerve firing rate. To better understand the hydrodynamic theory, SS on the TB in DMT should be quantified. However, such quantitative investigations have yet been systematically performed.

SS on the TB in DMT is affected by a wide range of parameters due to the highly complex structure of the intradental innervation system. There exist significant differences between reported data on the parameters of intradental innervation system, including biological structures (e.g., DMT structure,[27–29] diameters of nerve fibril/bead,[13,15] and odontoblastic process (OP),[12]) dentinal fluid density/viscosity,[30] and DFF velocity.[8,10] It is thus necessary to perform the systematic parameter studies of the various parameters on SS.

To investigate quantitatively the hydrodynamic theory of dental pain, in this study, we developed a computational fluid dynamics (CFD) model of fluid flow through innervated DMT to quantify DFF-induced SS on nerve terminals located in the DMT. The model was used to explore the influences of the major parameters on the SS, including the dimensions of biological structures, OP movement, DFF velocity, fluid viscosity, and density. The results from this study could lead to a better understanding of the mechanisms underlying dental pain sensation in clinical procedures (e.g., dentine sensitivity testing[31] and dental restorative processes[21,22]).

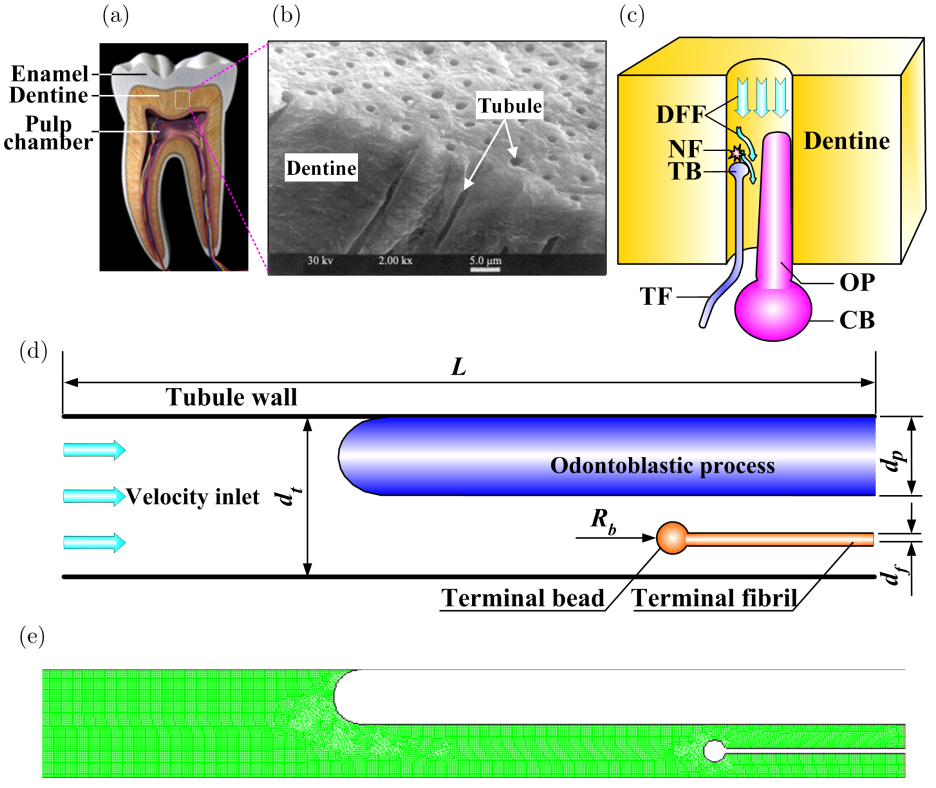

Fig. 1. Physiological relevant structures and meshing. (a) A cut-away image of human tooth illustrating composite layers (www.3dscience.com); (b) SEM image of dentine showing solid dentine material and the microtubules running perpendicularly from pulpal wall toward the dentine–enamel junction[11]; (c) schematic of typical dentine microtubule (DMT) structure and inward (toward the pulp) DFF through DMT causing sufficient SS on terminal bead (TB) and consequently neural firing (NF); (d) physically realistic model for fluid dynamics simulation; and (e) view of meshing. d_t, d_p, and d_f, are diameters of DMT, OP, and TF, respectively; R_b is radius of TB; L is computational length. Note that small terminal fibril (TF) could be detected lying in close relationship to the (OP),[12] whose cell body (CB) lies at the opening of the DMT at the pulp wall.[8] It was observed in most cases that only one TF inside the same DMT, accompanying only one OP.[13] One side of OP surface is in contact with tubular surface,[13] hence no dentinal fluid is allowed to pass through at this side. The TF and OP are modeled as rigid structure that do not deform due to DFF. We assumed that there is no synaptic structure between OP and TF,[14] though different finding has been reported.[13] TB that contains varying amounts of receptor organelles[15] is assumed as the sensory zone at the end of TF. The volume of TF is smaller as compared with odontoblast,[13] hence movements of TF as caused by DFF is negligible.

2. Mathematical Modeling

2.1. *Physical model of DMT innervation system*

Tooth is a sensory tissue with DMTs radiating throughout dentine from pulp wall to exterior cementum or dentine–enamel junction.[25] Whilst 40% of the DMTs located

in pulpal horn is innervated, the percentage is reduced to 8% in tooth crown and 1% in tooth neck.[12,15] The innervation system of tooth is composed of odontoblasts, nerve endings, and the liquid content of DMTs.[32] The unmyelinated nerve terminals (beaded fibrils) penetrate approximately 100–150 μm into the DMTs from pulpal wall.[12] In most cases, one DMT contains only one beaded fibril.[12] The DMT is also penetrated with OP (extension of an odontoblast), whose cell body lies at the pulp wall.[8] The outline of OP is smooth and not beaded.[12] Small beaded fibrils lying between OP and DMT wall have been observed.[12] Generally, there are one terminal fibril and one OP within the same DMT.[13] Based on these biological features stated above, the DMT structure and its innervation as well as the "hydrodynamic theory" are schematically shown in Fig. 1(c), where DFF through the DMT causes SS on the beaded nerve ending, activating thence nerve firing.

The geometrical dimensions of the various biological structures (e.g., DMT, terminal fibril, OP, and TB) of the intradental innervation system vary significantly by species and position within the tooth,[33] as listed in Table 1. The properties of dentinal fluid filling DMTs are summarized in Table 2.

2.2. *Computational model*

Although SS around TB wall may vary, the maximum SS (MSS), τ, is correlated with pain intensity. Hence, our CFD model was used to calculate the MSS on the TB (TB MSS) by solving the Navier–Stokes equation using commercially available CFD code (Fluent 6.3). Based on the *in vivo* DMT innervation system as described above and given the symmetrical structure of TB and OP in the longitudinally sectioned

Table 1. Structural parameters of intradental innervation system.

Parameter	Structure	Value	Reference
Diameter (μm)	Dentinal microtubule	2–4*	[25, 27–29]
	Dentinal microtubule	0.6–0.9◇	[25, 29]
	Dentinal microtubule	1.7⋆	[27, 28]
	Terminal fibril	0.32–0.02	[13]
	Terminal fibril	<0.2	[12]
	Terminal fibril (cat)	0.1	[34]
	Terminal bead	0.4–0.8	[12]
	Terminal bead	0.2–2	[15]
	Odontoblast process	<1	[12]
Length (extending from pulp wall into dentine microtubule, μm)	Nerve ending	100–200	[35]
	Nerve ending (cat)	100	[34]
	Nerve ending	150–200	[13]
	Nerve ending	1–200	[15]
	Odontoblast process	∼500△	[33,36]

*Near pulpal wall.
◇Near dentine–enamel junction.
⋆Below dentine–cementum junction.
△The extension of OP was found to be restricted to the inner half DMT.[34]

Table 2. Properties of dentinal fluid.

Parameter	Value	Reference
Flow velocity (μm/s)	27	[10]
	64	[10]
	400	[10]
	31.7–222.9	[8]
	211.4–369.6	[8]
	1200▲	[35]
Density (kg/m^3)	1005*	[30]
	1010#	[30]
Viscosity ($\times 10^{-3}$ Pa·s)	1.10*	[30]
	1.55#	[30]
	10△	[37]

▲Calculated velocity (≈369.6/30%) with consideration of 30% of tubules are in free communication with pulp.[38]
*Assumed as synovial fluid.
#Assumed as cerebrospinal fluid.
△Assumed as whole-blood viscosity.
Note that different intensity of thermal stimulation will cause different range of flow velocities as can be found from literatures.[8,37]

plane (along their axes), the 3D structure of innervated DMT was simplified to a two-dimensional (2D) model (Fig. 1(d)). Since we are only interested in the TB MSS, this simplification gives good approximation for fluid dynamics simulation. The terminal fibril and OP were modeled as rigid structure that do not deform due to DFF. The dentinal fluid was modeled as an incompressible and homogeneous Newtonian fluid. Steady state Navier–Stokes equations for incompressible fluids were employed, given by:

$$\nabla \bullet \mathbf{V} = 0 \tag{1}$$

$$\rho\,(\mathbf{V} \bullet \nabla)\,\mathbf{V} = -\nabla p + \mu \nabla^2 \mathbf{V}, \tag{2}$$

where $\mathbf{V}$ (m/s) and p (Pa) are the velocity vector and pressure of the fluid, respectively; ρ(kg/m^3) and μ(Pa $\cdot$ s) are the density and viscosity of the fluid, respectively.

A constant flow velocity was applied for the inlet boundary condition whilst the outflow condition was used at the outlet. The computational domain was meshed with rectangular elements and the element size of 0.035 μm was chosen based on mesh independence study. For wall SS distribution, the mesh was refined (element size 0.01 μm) in the region near the TB wall (Fig. 1(e)). The parameters used for the computational model are given in Table 3.

With the developed CFD model, we performed systematic parameter studies, with one parameter varying in a given range and other parameters fixed. The parameters selected were geometrical dimension of biological structure (λ), DFF velocity (V), dentinal fluid density (ρ) and viscosity (μ), and Reynolds number (Re).

Table 3. List of parameters and control values for computational model.

Parameter	Value
Flow velocity V (μm/s)	200
	400*
	600
	800
	1200
Dimensionless size of biological structure λ	0.05
	0.1
	0.15*
	0.25
	0.35
Dentinal fluid density ρ (kg/m^3)	1000
	1100*
	1200
	1300
	1500
Dentinal fluid viscosity μ ($\times 10^{-3}$ Pa·s)	1
	1.5*
	2.5
	5
	10
Computational length L(μm)	20
Computational length for OP (μm)	10
Computational length for TF (μm)	5

*Control value selected for computational model when studying influence of other parameters. Note that λ is defined as ratio of minimum space (between TB and OP) for DFF to maximum cross-sectional area (DMT diameter): $\lambda = \frac{d_t - d_p - 2R_b}{2d_t}$, where d_t (μm) and d_p (μm) are separately diameters of DMT and OP, R_b (μm) is radius of TB.

2.3. *Consideration of slip boundary effect*

In classical fluid dynamics (i.e., Eqs. (1)–(2)), nonslip boundary condition is assumed (i.e., zero relative fluid flow velocity at solid surface) at the interface between fluid and solid wall. This assumption provides good approximation when dealing with macroscale fluid behavior. However, when it comes to nano/microscale, this assumption can lead to great discrepancy compared with the more realistic slip boundary condition,[39] as noticeable slip of liquid at solid microchannel wall has been observed at this scale level.[40,41] The slip length is defined as the distance from the crest of the solid surface to the depth at which the linearly extrapolated velocity reaches zero. The slip length of water flow over solid surface in microchannels has been reported to vary in the range of ∼30 nm to ∼140 nm, depending on the diameter of the microchannel (∼3 μm to ∼11 μm) and the solid surface texture.[42] Table 3 shows that the channel diameter between OP and nerve fibril is about hundreds of nanometers. Consequently, the slip boundary effect of fluid flow in dentine tubes

on TB MSS should be considered. To this end, we correct the TB MSS obtained from the macrofluid behavior (nonslip boundary condition) as[40]:

$$\frac{\tau_{\text{slip}}}{\tau_{\text{nonslip}}} = \frac{1}{1 + (\frac{\delta}{h})}, \tag{3}$$

where τ_{slip} (Pa) and τ_{nonslip} (Pa) are the SS at a wall when slip and nonslip boundary conditions are applied, respectively; δ (μm) is the slip length (the slip length is defined as the distance from the crest of the solid surface to the depth at which the linearly extrapolated velocity reaches zero[42]) at the wall; and h (μm) is the distance between two parallel walls (e.g., local cross-sectional diameter).

3. Results and Discussion

3.1. *SS distribution and slip boundary effect*

First, the SS distribution on the TB and slip boundary effect was presented. A typical SS distribution on the TB is shown in Figs. 2(a)–2(b), with flow conditions as: the fluid viscosity and density were 1100 kg/m^3 and 0.0015 Pa $\cdot$ s; the dimensionless size of biological structure was 0.15; the velocity of the fluid was 400 μm/s (all were taken as control values as summarized in Table 3). It is found that the maximum value of the SS on the TB wall appears on the place of minimal cross-sectional area (Fig. 2(b)). Equation (3) identifies the difference between the SS when slip and nonslip boundary conditions are applied. $\tau_{\text{slip}}/\tau_{\text{nonslip}} \approx 0.83$ when $\delta = 0.1\mu$m[42] and $h = 0.5\,\mu$m (an average value taken form Table 1), indicating huge difference between the two results that confirms the necessity of considering nonslip boundary condition at the wall.

3.2. *Effect of DFF velocity*

Noxious stimulation (e.g., thermal/mechanical loading, dental restorative processes) on tooth cause DFF in DMT,[8,21,22] and a larger stimulation intensity may result in a higher DFF velocity.[31,43] The DFF velocity has been correlated with intradental nerve firing rate, although the transduction mechanism is not yet clear.[8,10] Matthews and Vongsavan[44] postulated that the DFF velocity may produce sufficiently large SS on the TB, opening the mechanosensitive ion channels in the cell membranes (i.e., TB wall) and thereby exciting these channels.

To explore the relationship between DFF velocity and TB MSS, we performed simulation under boundary conditions of different velocities (Table 3) to calculate the corresponding TB MSS (Fig. 3(a)). We observed that the TB MSS increases linearly with increasing fluid velocity, e.g., MSS is increased from 21.1 Pa to 132.5 Pa when the velocity is increased from 200 μm/s to 1200 μm/s. It has been reported that low-threshold intradental mechanoreceptors are sensitive to disturbance induced by gently touching the dentine surface with a fine glass

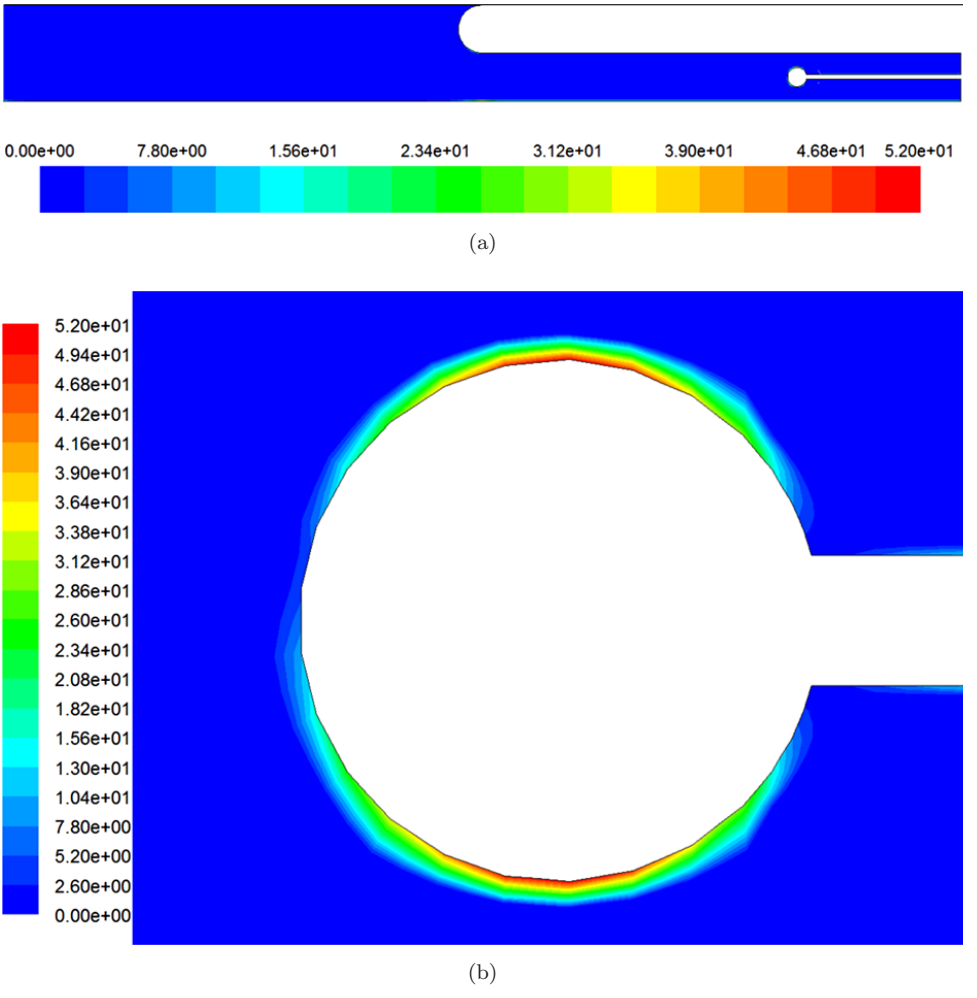

Fig. 2. Simulated SS contour: (a) typical SS contour for the CFD model with flow conditions taken as control values; and (b) an enlarged picture for the SS distribution around the TB wall.

probe,[45] although the exact threshold value has not been experimentally determined. The lowest threshold for mechanoreceptors in human lingual nerve was reported to be ∼150 Pa.[46] Under the present simulation conditions, the values of TB MSS from our simulation (Figs. 3(a)–3(e)) are at a comparable level (25–300 Pa), which may, therefore, cause dental pain sensation.[8,10] The increase of TB MSS with increasing fluid velocity agrees well with existing experimental observations (a higher TB MSS evokes a higher pain intensity, in other words, higher nerve firing rate).[8,10] This confirms the postulation of Matthews and Vongsavan[44]: at an elevated fluid velocity, the TB MSS may exceed the threshold of intradental mechanoreceptors, causing thereby neural firing.

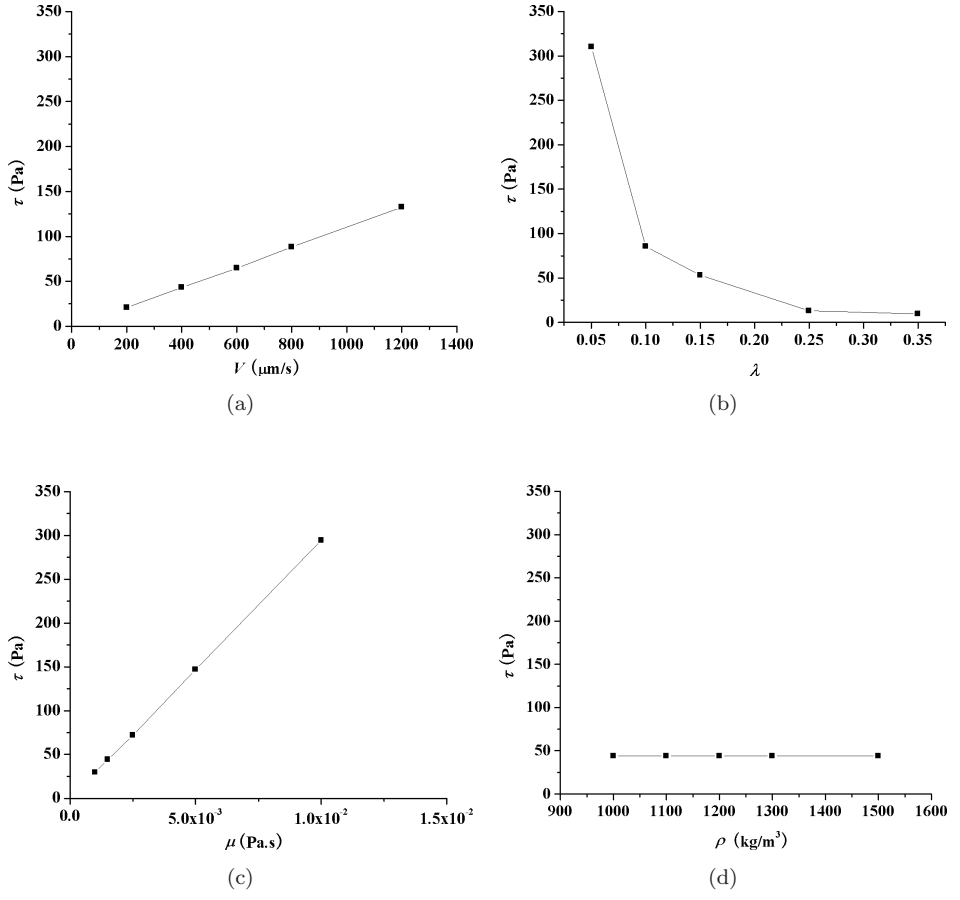

Fig. 3. Effects of various parameters on TB MSS for selected parameters of control values. (a) Effect of DFF velocity; (b) effect of dimensionless size of biological structure λ; (c) effect of dentinal fluid viscosity and (d) effect of dentinal fluid density.

3.3. *Effect of biological structure*

The diameters of DMT, terminal fibril, OP, and TB vary significantly in different species and are strongly dependent upon their positions within tooth[33] (Table 1). In addition, the inward (toward the pulp chamber) DFF has been observed to cause a slightly movement of OP toward the pulp chamber.[8] Since OP diameter varies along its longitudinal direction,[13] the OP movement changes the dimension of the space for the DFF, thus affecting the SS on the TB.[25] The effect of the OP movement upon the TB MSS is taken into account by varying the value of d_p. Movement of terminal fibril can be neglected due to its small volume as compared with odontoblast.[13,25] To account for the combined effect of these biological structures, a dimensionless geometrical parameter λ is introduced, defined as the ratio of the minimum space

(between the TB and the OP) for DFF to the maximum cross-sectional area (DMT diameter; see Fig. 1(d)):

$$\lambda = \frac{d_t - d_p - 2R_b}{2d_t}, \tag{4}$$

where d_t (μm) and d_p(μm) are separately the diameter of the DMT and the OP, and R_b (μm) is the radius of TB.

λ is shown to significantly affect the TB MSS (Fig. 3(b)). With TB MSS increases from 9.5 to 310.5 Pa when λ is reduced from 0.35 to 0.05. Note that, as the value of λ is reduced, the local channel for DFF becomes narrower. With a constant inlet velocity, reducing the cross-sectional area leads to increased flow velocity across the TB (due to mass conservation), hence resulting in a larger TB MSS (and hence a higher pain intensity).[8,10] Given the complexity of tooth biological structures and their strong influence on TB MSS, the present results indicate that dental pain study of animal models may not be directly applied to human being and the results may even vary from one person to another. Besides, as reflected in the change of d_p values and thus the change in λ, OP movement due to DFF also affect the predicted TB MSS. The OP movement-induced change in TB MSS explains the phenomenon that cold stimulation evokes sharper and more shooting pain sensations than hot stimulation.[26]

3.4. *Effect of dentinal fluid viscosity*

To check the effect of fluid viscosity on the TB MSS, dentinal fluid viscosity, 0.0015 Pa·s (resembling cerebrospinal fluid[30]), is taken as the control value. The lower limit of the viscosity is assumed to be identical to that of plasma (0.001 Pa·s), while the upper limit is assumed to be the same as blood (0.01 Pa·s). The predicted effect of fluid viscosity on TB MSS is plotted in Fig. 3(c). It can be seen that TB MSS increases with increasing fluid viscosity. The effect appears to be significant. We postulate that dentinal fluid viscosity may increase in inflamed pulp. Hence, a tiny fluid flow in DMT may cause sufficient TB MSS (due to increased fluid viscosity) triggering the intradental mechanoreceptors, resulting in dental pain. This may provide an alternative explanation for the hypersensitivity in inflamed pulp. Besides, the variation of temperature also affects dentinal fluid viscosity. For example, when tooth is cooled, the dentinal fluid viscosity increases significantly (46% increase in water viscosity when cooled from 25 to 10°C),[47] resulting in increased TB MSS. Tooth heating will do the reverse due to the decrease in viscosity.[25]

3.5. *Effect of dentinal fluid density*

Dentinal fluid, with similar composition to plasma, has been described as transparent and cell-less. For example, Knutsson *et al.*[48] found that dentinal fluid contains plasma protein, such as fibrinogen and albumin. The physical properties of dentinal fluid are taken as similar to that of synovial or cerebrospinal fluid, even though

small differences in chemical composition may exist.[30] We assume that the density of dentinal fluid has a upper limit of 1500 kg/m^3 (larger than blood density, 1060 kg/m^3), which is ∼50% larger than the control value, 1010 kg/m^3 (taken here as identical to that of cerebrospinal fluid). The lower limit is taken as identical to that of plasma, 1000 kg/m^3. Figure 3(d) shows the effect of fluid density on the predicted TB MSS. The TB MSS remains unchanged (∼44.2 Pa) when the fluid density varies from 1000 to 1500 kg/m^3, which indicates the negligible influence of fluid density on the TB MSS.

3.6. *Effects of combined factors*

To determine the effects of combinational factors on TB MSS, the Reynolds number (Re $= \rho V d_t/\mu$) is used to consider simultaneously the effects of DFF velocity (V), dentinal fluid density (ρ) and viscosity (μ), and characteristic length (DMT diameter, d_t). For convenience, the TB MSS (τ) is nondimensionalized as $\tau^* = \tau/(0.5\,\rho u^2)$. Figure 4 shows the combinational effects of all factors, and τ^* decreasing with increasing Re for a selected value of λ is observed. This trend becomes more significant when a lower value of λ is considered, indicating the combined effect of DFF velocity and fluid density/viscosity will have significant influence on τ^* when the representative size of biological structures λ is small. Figure 4 also reveals that, for a specific Re, τ^* decreases with increasing λ which is consistent with the results shown in Fig. 3(b). This trend becomes more significant when Re is typically small.

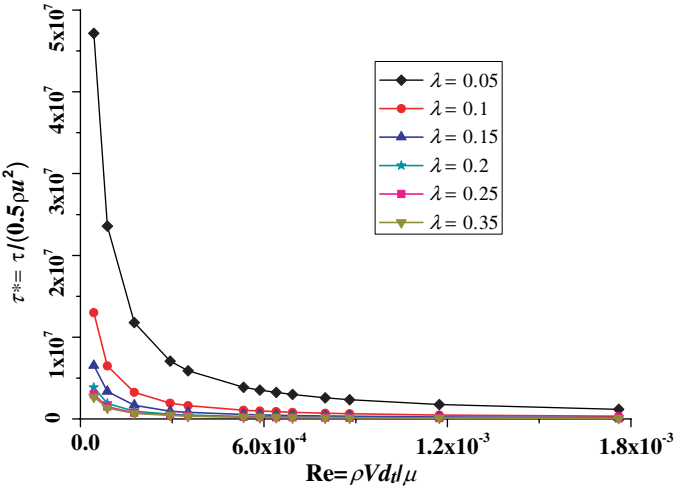

Fig. 4. Effect of Reynolds number. Note that Reynolds number (Re $= \rho V d_t/\mu$) is a combined factor that accounts for DFF velocity (V), dentinal fluid density (ρ) and viscosity (μ), and characteristic length (DMT diameter, d_t).

4. Conclusions

In this study, we developed a CFD model to study DFF in innervated DMT and performed parametric analysis of TB MSS. The dimensions of biological structures, OP movement, DFF velocity, fluid viscosity, and the Reynolds number were found to have significant influence on TB MSS, while the dentinal fluid density showed negligible influences. Our simulations indicate that animal dental pain models may not be directly applied to human being and the results may even vary from one person to another. Changes of dentinal DFF velocity due to temperature variation and inflammation may have significant influences on the TB MSS and, consequently, dental pain intensity. These results quantitatively confirm the hydrodynamic theory of dental pain. The simulation results here also imply that: (1) in case of exposed dentine (the enamel layer is worn out), dental pain could be effectively prevented by sealing the dentinal tubules reducing the fluid flow velocity and (2) since thermal stimulation causes significant DFF,[8,31] dental thermal pain mechanism may also involve in DFF-induced SSs on nerve endings.

In future studies, it would be of great significance to quantitatively investigate the mechanoreceptor transduction process in dental pain sensation induced by DFF. This could offer mechanistic insight into some enigmatic experimental observations, e.g., the intradental mechanoreceptors are not "equally sensitive" to inward (toward the pulp) and outward (away from the pulp) DFF, thereby, explain theoretically the differences between hot and cold dental pain responses.

List of abbreviations

SS, shear stress; CFD model; computational fluid dynamics model; DFF, dentinal fluid flow; DMTs, dentinal microtubules; TB, terminal beads; OP, odontoblastic process; MSS, maximum shear stress; TB MSS, maximum shear on the TB; TF, terminal fibril; CB, cell body.

Conflict of interest statement

None.

Acknowledgment

This work was supported by the National Natural Science Foundation of China (10825210, 31050110125, 81000453) and the National 111 Project of China (B06024).

References

1. Lin M, Xu F, Lu TJ, Bai BF, A review of heat transfer in human tooth — Experimental characterization and mathematical modeling, *Dent Mater* **26**(6):501–513, 2010.

2. Fahey M, Onyejekwe O, Lawrence Mason H, Mitra K, Precise dental ablation using ultra-short-pulsed 1552 nm laser, *Int J Heat Mass Trans* **51**(23–24):5732–5739, 2008.
3. Rode AV, Gamaly EG, Luther-Davies B, Taylor BT, Graessel M, Dawes JM, Chan A, Lowe RM, Hannaford P, Precision ablation of dental enamel using a subpicosecond pulsed laser, *Aust Dent J* **48**(4):233–239, 2003.
4. Uhl A, Mills RW, Jandt KD, Polymerization and light-induced heat of dental composites cured with LED and halogen technology, *Biomaterials* **24**(10):1809–1820, 2003.
5. Hannig M, Bott B, *In-vitro* pulp chamber temperature rise during composite resin polymerization with various light-curing sources, *Dent Mater* **15**(4):275–281, 1999.
6. Bouillaguet S, Caillot G, Forchelet J, Cattani-Lorente M, Wataha JC, Krejci I, Thermal risks from LED- and high-intensity QTH-curing units during polymerization of dental resins, *J Biomed Mater Res Part B* **72B**(2):260–267, 2005.
7. Sessle BJ, Invited review: The neurobiology of facial and dental pain: Present knowledge, future directions, *J Dent Res* **66**(5):962–981, 1987.
8. Andrew D, Matthews B, Displacement of the contents of dentinal tubules and sensory transduction in intradental nerves of the cat, *J Physiol* **529**(3):791–802, 2000.
9. Charoenlarp P, Wanachantararak S, Vongsavan N, Matthews B, Pain and the rate of dentinal fluid flow produced by hydrostatic pressure stimulation of exposed dentine in man, *Arch Oral Biol* **52**(7):625–631, 2007.
10. Vongsavan N, Matthews B, The relationship between the discharge of intradental nerves and the rate of fluid flow through dentine in the cat, *Arch Oral Biol* **52**(7):640–647, 2007.
11. Grayson W, Marshall J, Dentin: Microstructure and characterization, *Ouint lnt* **24**(9):606–617, 1993.
12. Fearnhead RW, Histological evidence for the innervation of human dentine, *J Anat* **91**(Pt 2):267–277, 1957.
13. Carda C, Peydro A, Ultrastructural patterns of human dentinal tubules, odontoblasts processes and nerve fibres, *Tissue Cell* **38**(2):141–150, 2006.
14. Ibuki T, Kido MA, Kiyoshima T, Terada Y, Tanaka T, An ultrastructural study of the relationship between sensory trigeminal nerves and odontoblasts in rat dentin/pulp as demonstrated by the anterograde transport of wheat germ agglutinin-horseradish peroxidase (WGA-HRP), *J Dent Res* **75**(12):1963–1970, 1996.
15. Byers MR, Dental sensory receptors, *Int Rev Neurobiol* **25**:39–94, 1984.
16. Brännström M, The hydrodynamic theory of dentinal pain: sensation in preparations, caries, and the dentinal crack syndrome, *J Endod* **12**(10):453–457, 1986.
17. Brännström M, Aström A, The hydrodynamics of the dentine; its possible relationship to dentinal pain, *Int Dent J* **22**(2):219–227, 1972.
18. Brännström M, Johnson G, The sensory mechanism in human dentin as revealed by evaporation and mechanical removal of dentin, *J Dent Res* **57**(1):49–53, 1978.
19. Brännström M, Linden LA, Astrom A, The hydrodynamics of the dental tubule and of pulp fluid. A discussion of its significance in relation to dentinal sensitivity, *Caries Res* **1**(4):310–317, 1967.
20. Trowbridge HO, Franks M, Korostoff E, Emling R, Sensory response to thermal stimulation in human teeth, *J Endod* **6**(1):405–412, 1980.
21. Ratih DN, Palamara JEA, Messer HH, Dentinal fluid flow and cuspal displacement in response to resin composite restorative procedures, *Dent Mater* **23**(11):1405–1411, 2007.
22. Kim S-Y, Ferracane J, Kim H-Y, Lee I-B, Real-time measurement of dentinal fluid flow during amalgam and composite restoration, *J Dent* **38**(4):343–351, 2010.

23. Lin M, Liu SB, Niu L, Xu F, Lu TJ, Analysis of thermal-induced dentinal fluid flow and its implications in dental thermal pain, *Arch Oral Biol*, 2011, DOI: 10.1016/j.archoralbio.2011.02.011.
24. Brännström M, Astroem A, A study on the mechanism of pain elicited from the dentin, *J Dent Res* **43**:619–625, 1964.
25. Pashley DH, Dynamics of the pulpo-dentin complex, *Crit Rev Oral Biol Med* **7**(2):104–133, 1996.
26. Lin M, Luo ZY, Bai BF, Xu F, Lu TJ, Fluid mechanics in dentinal microtubules provides mechanistic insights into the difference between hot and cold dental pain, *PLoS ONE*, 2011, DOI: 10.1371/journal.pone.0018068.
27. Franquin JC, Remusat M, Abou I, Dejou J, Immunocytochemical detection of apoptosis in human odontoblasts, *Eur J Oral Sci* **106**:384–387, 1998.
28. Vermelin L, Lecolle S, Septier D, Lasfagues JJ, Goldberg M, Apoptosis in human and rat dental pulp, *Eur J Oral Sci* **104**:547–553, 1996.
29. Garberoglio R, Brännström M, Scanning electron microscopic investigation of human dentinal tubules, *Arch Oral Biol* **21**(6):355–362, 1976.
30. Berggren G, Brännström M, The rate of flow in dentinal tubules due to capillary attraction, *J Dent Res* **44**(2):408–415, 1965.
31. Linsuwanont P, Palamara JEA, Messer HH, An investigation of thermal stimulation in intact teeth, *Arch Oral Biol* **52**(3):218–227, 2007.
32. Gillam DG, Mordan NJ, Newman HN, The dentin disc surface: a plausible model for dentin physiology and dentin sensitivity evaluation, *Adv Dent Res* **11**(4):487–501, 1997.
33. Holland GR, The odontoblast process: form and function, *J Dent Res* **64**:499–514, 1985.
34. Holland GR, Matthews B, Robinson PP, An electrophysiological and morphological study of the innervation and reinnervation of cat dentine, *J Physiol* **386**:31–43, 1987.
35. Byers MR, Narhi MVO, Dental injury models: experimental tools for understanding neuroinflammatory interactions and polymodal nociceptor functions, *Crit Rev Oral Biol Med* **10**(1):4–39, 1999.
36. Thomas HF, The dentin-predentin complex and its permeability: anatomical overview, *J Dent Res* **64**(Special Issue):607–612, 1985.
37. Shin S, Ku YH, Park MS, Suh JS, Measurement of blood viscosity using a pressure-scanning capillary viscometer, *ClinHemorheo Microcirc* **30**(3):467–470, 2004.
38. Pashley DH, Livingston MI, Reeder OW, Horner JA, Effects of the degree of tubule occlusion on the permeability of human dentine, *in vitro*, *Arch Oral Biol* **23**:1127–1133, 1978.
39. Lee YH, Sin H-C, Kim NW, Impact of slip and contact angle on imprinting pressure in nanoimprint lithography, *J Vacu Sci Technol B* **27**(2):590–596, 2009.
40. Choi C-H, Kim C-J, Large slip of aqueous liquid flow over a nanoengineered superhydrophobic surface, *Phys Rev Lett* **96**:066001, 2006.
41. Joseph P, Cottin-Bizonne C, Benoît JM, Ybert C, Journet C, Tabeling P, Bocquet L, Slippage of water past superhydrophobic carbon nanotube forests in microchannels, *Phys Rev Lett* **97**:156104, 2006.
42. Choi C-H, Ulmanella U, Kim J, Ho C-M, Kim C-J, Effective slip and friction reduction in nanograted superhydrophobic microchannels, *Phys Fluids* **18**(8):087105–087108, 2006.
43. Paphangkorakit J, Osborn JW, The effect of normal occlusal forces on fluid movement through human dentine *in vitro*, *Arch Oral Biol* **45**(12):1033–1041, 2000.

44. Matthews B, Vongsavan N, Interactions between neural and hydrodynamic mechanisms in dentine and pulp, *Arch Oral Biol* **39**(Suppl):S87–S95, 1994.
45. Matthews B, Peripheral and central aspects of trigeminal nociceptive systems, *Philo Trans R Soc Lond B* **308**(1136):313–324, 1985.
46. Trulsson M, Essick GK, Low-threshold mechanoreceptive afferents in the human lingual nerve, *J Neurophysiol* **77**(2):737–748, 1997.
47. Pashley DH, Thompson SM, Stewart FP, Dentine permeability: effects of temperature on hydraulic conductance, *J Dent Res* **62**(9):956–959, 1983.
48. Knutsson G, Jontell M, Bergenholtz G, Determination of plasma proteins in dentinal fluid from cavities prepared in healthy young human teeth, *Arch Oral Biol* **39**(3):185–190, 1994.